ISSN 1990-7931, Russian Journal of Physical Chemistry B, 2024, Vol. 18, No. 2, pp. 607–623. © Pleiades Publishing, Ltd., 2024.

CHEMICAL PHYSICS OF NANOMATERIALS

Nanomaterials for Sustainable Energy in Hydrogen-Fuel Cell: Functionalization and Characterization of Carbon Nano-Semiconductors with Silicon, Germanium, Tin or Lead through Density Functional Theory Study

F. Mollaamin[a], * and M. Monajjemi[b]

[a] *Department of Biomedical Engineering, Faculty of Engineering and Architecture, Kastamonu University, Kastamonu, Turkey*
[b] *Department of Chemical Engineering, Central Tehran Branch, Islamic Azad University, Tehran, Iran*
**e-mail: smollaamin@gmail.com*

Received November 7, 2023; revised December 11, 2023; accepted December 20, 2023

Abstract—Hydrogen fuel is a promising route to remark on the energy and environmental challenges facing the world today. Therefore, hydrogen storage has become enhancing essential for progressing cleaner and more sustainable technologies. Recent research has recognized metal and metalloid hydrides as a promising alternative that might suggest some benefits over compressed storage. In this work, a profound study on the adsorption of hydrogen by nanocone carbides of main group elements including Si, Ge, Sn and Pb has been done including both geometrical and electronic properties using density functional calculations. The effect of substituting silicon (Si) in silicon carbide by germanium (Ge), tin (Sn) or lead (Pb) elements on the geometrical structure and H atom adsorption behavior were investigated. The results show that when Si atoms are replaced by a Ge, Sn or Pb atoms, the hydrogen adsorption energy is greatly enhanced. Thermochemical, electric and magnetic properties of SiC, GeC, SnC and PbC nanocones and SiC–6H, GeC–6H, SnC–6H and PbC–6H nanocones hydrides are studied by the first-principles methods based on the density functional theory for adsorbing hydrogen atoms. The assumption of the chemical adsorption has been approved by the projected density of states and charge density difference plots. Charge density difference calculations also indicate that the electronic densities were mainly accumulated on the adsorbate of hydrogen atoms. Therefore, these results indicate that the SiC, GeC, SnC and PbC nanocones can be considered as good candidates for hydrogen adsorption and might be helpful for fabricating nano-devices such as hydrogen storage nanomaterials.

Keywords: energy storage, nanomaterial carbides, adsorption, density functional theory

DOI: 10.1134/S1990793124020271

INTRODUCTION

Hydrogen might be produced from natural gas, nuclear power, biomass, and sustainable power like solar and wind. These specifications build it a favorable fuel for energy generation and transportation. It may also be applied in cars, homes, portable power like microgrids, and different applications [1–3]. Incorporating hydrogen cells, batteries, and supercapacitors through designing an energy storage system can conclude in the demanded functioning [4].

Carbon nanotubes due to their light mass density, cylindrical structure, high surface to volume ratio, as well as high degree of reactivity between the carbon and hydrogen has been suggested for hydrogen storage [5, 6]. Moreover, it is well known that the adsorption of hydrogen by carbon nanotubes is temperature dependent, which can be impressively utilized for hydrogen adsorption. Many theoretical and experimental studies have been concentrated on hydrogen storage in carbon nanotubes [7, 8].

Scientists proposed that hydrogen storage on carbon nanomaterial deals with dissociation of molecular hydrogen. The dissociation of hydrogen takes place at transition metal sites, which are present due to residues of transition metals in the nanomaterial samples [9–11]. Graphene with two-dimensional (2D) layered physical structure and the unique electronic properties has simulated a broad range of research enthusiasm on 2D materials which can be applied for the electronic, optoelectronic, and spintronic devices [12–16]. But the practical application of 2D material like graphene might be confined with small band gap. Thus, new 2D materials with perfect mechanical, thermoelectric, optical and electronic properties are the clue to the recent scientific investigations [17–20].

In transition metal (TM) decorated carbon nanostructure, the TM-carbon binding takes place through

a charge-transfer mechanism and the TM remains in the cationic state. Therefore, the gas molecule can get absorbed on the cationic transition metal element giving some electronic charge [21–24]. In addition, transition metal (TM) atoms are the source of magnetism; in the results of TM-doped SiC monolayer, it can be found that the system can be a magnetic semiconductor by Co, Cu, Fe, Mn, and Ni doping [25]. The TM dopants can cause a total Hamiltonian perturbation, eventually leading to changes in electronic structures, which makes it a substantial application in magnetic electronic devices [26–32]. Carbon nanocones are one of the nanomaterials which have structures close to carbon nanotubes with properties much like carbon nanotubes [33–36].

Meanwhile, owing to the fast progress in SiC technology, the crystalline structure of this material could be regarded to contain the close-packed stacking of two layers of silicon (Si) and carbon (C) atoms. Each C or Si atom is closed by four Si or C atoms in intense tetrahedral $sp3$ bonds with about 3.08 Å of distance between neighbor atoms of Si and C [37]. It is known that for optimum adsorption of gas molecules, the ideal form of binding between the host material (SiC nanosheet) and adsorbed gas molecules should be intermediate between physisorption and chemisorption energy [38].

In this research, we shall present the theoretical estimates for the charge transfer and the energy of binding with the SiC, GeC, SnC and PbC nanocones for adsorption of all hydrogen atoms (six hydrogens) (Figs. 1a–1d). Then, it investigated the magnetic and electronic structures of SiC–6H, GeC–6H, SnC–6H and PbC–6H nanocone hydrides. With continued investment and research, metal and metalloid hydrides could play a key role in realizing the full potential of hydrogen fuel and contributing to a more sustainable future [39, 40].

Metals and metal alloys can absorb hydrogen in their molecular state, therefore functioning as hydrogen sponges. Various metallic atoms have different degrees of hydrogen absorption, resulting in a diverse variety of hydrogen storage materials which may have a higher hydrogen storage density even than hydrogen gas. Thus, metal hydride storage enables the safe and volume-efficient storage of hydrogen for onboard vehicle applications [41–43].

MATERIALS AND METHOD

It was reported that the most stable structure of planar SiC forms graphene-like structure with alternative SiC bond and the bonding in such structure is of sp^2 type [44]. In this article, nanocone carbides (1, 5) of Si, Ge, Sn and Pb have been modeled by disclination angle of 180°, cone height of 20 Å (Figs. 1a–1d). In our calculation, we have considered similar structure and optimized without any symmetry constraint.

The adsorbing of hydrogen atoms on the surface of SiC, GeC, SnC and PbC nanocones was defined by the theory Langmuir isotherm [45, 46], which indicates the chemisorption between 6H atoms and SiC, GeC, SnC and PbC nanocones using the GaussView 6.06.16 [47] and Gaussian 16 revision C.01 program package [48] and density functional theory (DFT) method [49–51].

The B3LYP hybrid density functional is very prosperous in the investigation of thermochemistry of atoms and molecules for solids and surfaces and reproduces the experimental energy gaps and magnetic moments for a variety of materials [52]. First, the contribution of HF exchange was dampened to zero at short range, a feature that counteracts other advantages of hybrid functionals, leading Yanai and coworkers to suggest a variation, the Coulomb-attenuated B3LYP (CAM-B3LYP) method in which the damping function was empirically optimized to deliver robust performance for a wider range of molecular properties [53]. The first relevant implementation of CAM-B3LYP into a code for materials-science modelling has just been reported, an implementation into the Car–Parrinello molecule dynamic package for gamma-point-only calculations. The results obtained demonstrated enhanced optical spectra prediction, as expected [54]. By increasing the investigation on metals and metalloids, the LANL2DZ basis set becomes one of the most popular basis sets for these complexes among others. The LANL2DZ with impressive core potential basis set was applied for all theoretical computations. This basis set exchanges the 1s through 2p electron of the atoms with a potential field for saving the number of calculations [55–59].

In this work, from the charge density distribution of the SiC sheet, it is seen that a considerable amount of electronic charge is transferred from Si, Ge, Sn, Pb to C site. The presence of these point charges on the SiC, GeC, SnC and PbC nanocones influences the 6H adsorption property.

Figures 1a–1d has shown that the SiC, GeC, SnC and PbC nanocones are distorted after adsorbing H atoms in such a way that H atoms can bind to Si, Ge, Sn, Pb atoms along with neighboring carbon atoms towards developing the stability of the system. When the H atom is adored by the SiC, GeC, SnC and PbC nanocones, the H–X (Si, Ge, S, Pb) bond distance is ≈1.5 Å and H–C is ≈1.1 Å. Although Si, Ge, S, Pb and C atoms are iso-valent, the most stable state of C is sp^2 and Si, Ge, S, Pb is sp^3.

The charge transfer between adsorbates of H atoms and adsorbents of SiC, GeC, SnC and PbC nanocones is calculated due to the Bader charge analysis [60]. This method can measure charge accumulation from the charge of each atom in the complex model. Finally, the total adsorption charge transfer can be obtained as formula: $\Delta Q_t = Q2 - Q1$, where Q_2 and Q_1 remark the charge of SiC, GeC, SnC and PbC nano-

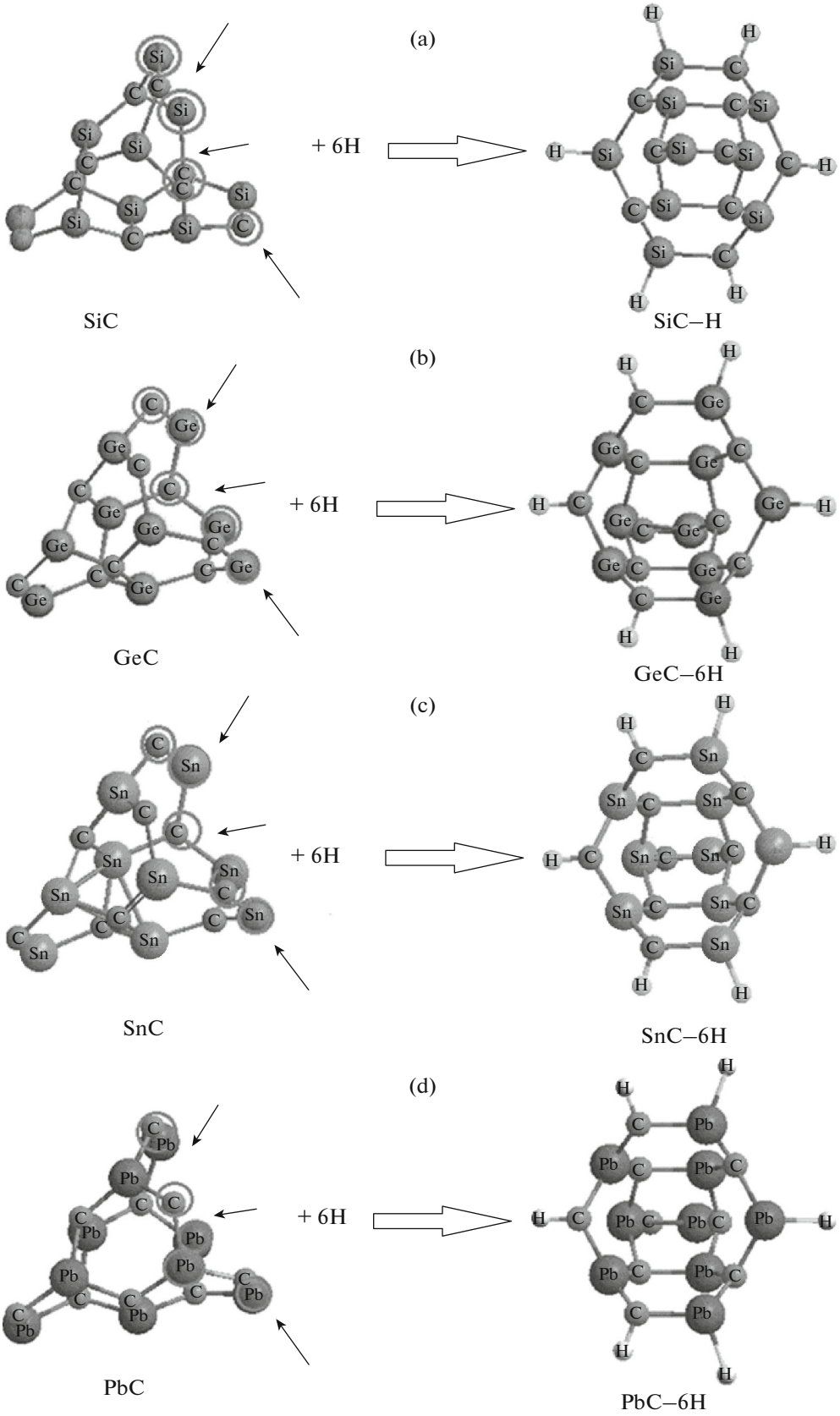

Fig. 1. Langmuir adsorption of hydrogen onto SiC, GeC, SnC, and PbC nanocones towards formation clusters of (a) SiC–6H, (b) GeC–6H, (c) SnC–6H, and (d) PbC–6H nanocone hydrides.

cones after and before adoption of H atoms, respectively. In fact, negative ΔQ_t indicates that electrons are transferred from H atoms to the surface of SiC, GeC, SnC and PbC nanocones, and the adsorbent acts as an electron acceptor [61, 62].

The changes of charge density analysis in the adsorption process have illustrated that SiC shows the Bader charge of –0.667e, before adsorption of 6H, and –0.674e after adsorption of 6H, respectively. GeC shows the Bader charge of –0.631e, before adsorption of 6H, and –0.652e after adsorption of 6H, respectively. SnC shows the Bader charge of –0.829e, before adsorption of 6H, and –0.858e after adsorption of 6H, respectively. PbC nanocone shows the Bader charge of –0.913e, before adsorption of 6H, and –0.923e after adsorption of 6H, respectively.

Therefore, the changes of charge density for Langmuir adsorption of H atoms on SiC, GeC, SnC and PbC nanocones alternatively are $\Delta Q_{6H \to SiC} = -0.007e > \Delta Q_{6H \to SnC} = -0.029e > \Delta Q_{6H \to GeC} = -0.021e > \Delta Q_{6H \to PbC} = -0.01e$. The values of changes of charge density have shown a more important charge transfer for SiC, GeC, SnC and PbC nanocones which act as the electron acceptor while H atoms as the stronger electron donors through adsorption on the SiC, GeC, SnC and PbC nanocones.

Different quantum chemical topology approaches, and Laplacian of electron density) on SiC4H2 isomers are employed to complement each other. The obtained results dictate that the lone pair of the silicon atom participates in delocalization and influences the structural stability of isomers [63].

RESULTS AND DISCUSSION

The Projected Density of States and Electronic Specifications

The appearance of the energy states (*p*-orbital) of Si and (*d*-orbital) of Ge, Sn, Pb within the gap of SiC, GeC, SnC and PbC nanocones induces the reactivity of the system. It is clear from that after adsorption of all hydrogen atoms (six hydrogens) by SiC, GeC, SnC and PbC nanocones, there is a significant contribution of Ge, Sn, Pb *d*-orbital in the unoccupied level. Based on the population analysis and the projected density of states (PDOS), it can be concluded that Si, Ge, Sn, Pb remain in the cationic state, and it can accept more electrons from other atoms.

Figures 2a–2d shows that the SiC–6H states have more contribution at the conduction band between –5 to –15 eV, while contribution of carbon sates is expanded, and silicon and hydrogen states have minor contributions. The nanocones of GeC–6H, SnC–6H, and PbC–6H, respectively, have more contribution at the middle of the conduction band between –5 to –10 eV, while contribution of carbon sates is expanded with major distribution approximately at –7 eV, and the main group metals of germanium, tin and lead states have less contributions compared to carbon.

Nuclear Quadrupole Resonance Spectra of 6H-adsorption Onto Nanocone Carbides

Nuclear quadrupole resonance (NQR) procedure has been done out for the complexes of all hydrogen atoms (six hydrogens) adsorbing on SiC, GeC, SnC and PbC nanocones is related to the multipole enlargement in cartesian harmonies as follows [64–67]. Since the electric field gradient at the situation of hydrogen atoms adsorbed on the SiC, GeC, SnC and PbC nanocones as the gas sensor is approved by the valence electrons distorted in the special connection with close nuclei of these nanocones, the nuclear quadrupole resonance at which transitions occur is SiC–6H, GeC–6H, SnC–6H, PbC–6H nanocones (Table 1).

Furthermore, in Figs. 3a–3d it has been drawn the electric potential of nuclear quadrupole resonance method versus Bader charge for elements of hydrogen, carbon, silicon, germanium, tin and lead in the adsorption process of hydrogen atoms on the SiC, GeC, SnC and PbC nanocones by CAM-B3LYP/EPR-III, 6-311+G(*d*, *p*), LANL2DZ theoretical level.

It has been observed the effect of the binding between hydrogen atoms with carbon, silicon, germanium, tin and lead in the SiC–6H, GeC–6H, SnC–6H, PbC–6H nanocones during adsorbing H atoms through resulted electric potential using NQR analysis (Figs. 3a–3d). It's obvious that the capability of SiC, GeC, SnC and PbC nanocones for detecting of H atoms is fluctuated by their selectivity and sensitivity which can represent the efficiency of these nanocones as the promising gas storage (Figs. 3a–3d). The curves deviations of SiC from SiC–6H, GeC from GeC–6H, SnC from SnC–6H, and PbC from PbC–6H nanocones, respectively, have demonstrated the effect of H-adsorption on the SiC, GeC, SnC and PbC nanocones (Figs. 3a–3d). Therefore, it can be suggested that applied carbides in this work can act as potential hydrogen storage device materials because of their higher hydrogen uptake capacity.

Nuclear Magnetic Resonance Spectra of 6H-adsorption Onto Nanocone Carbides

Shielding tensors of isotropic (σ_{iso}) and anisotropy (σ_{aniso}) extracted from nuclear magnetic resonance (NMR) spectroscopy for certain atoms in the active site of 6H–adsorbed on the SiC, GeC, SnC, PbC nanocones through the binding between hydrogen atoms and solid surfaces towards formation of SiC–6H, GeC–6H, SnC–6H, PbC–6H nanocones

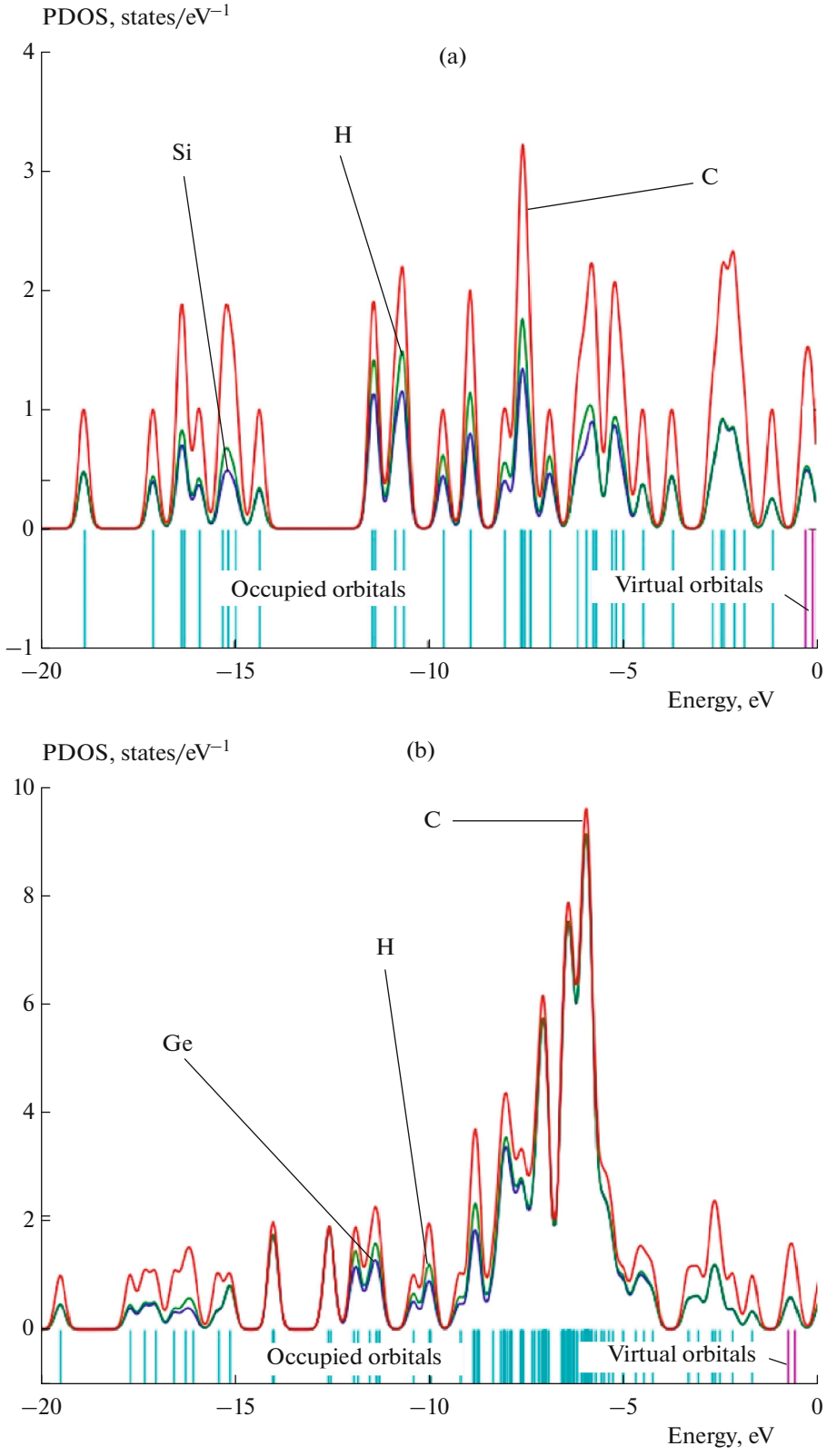

Fig. 2. PDOS adsorption of (a) SiC–6H, (b) GeC–6H, (c) SnC–6H, and (d) PbC–6H nanocone hydrides.

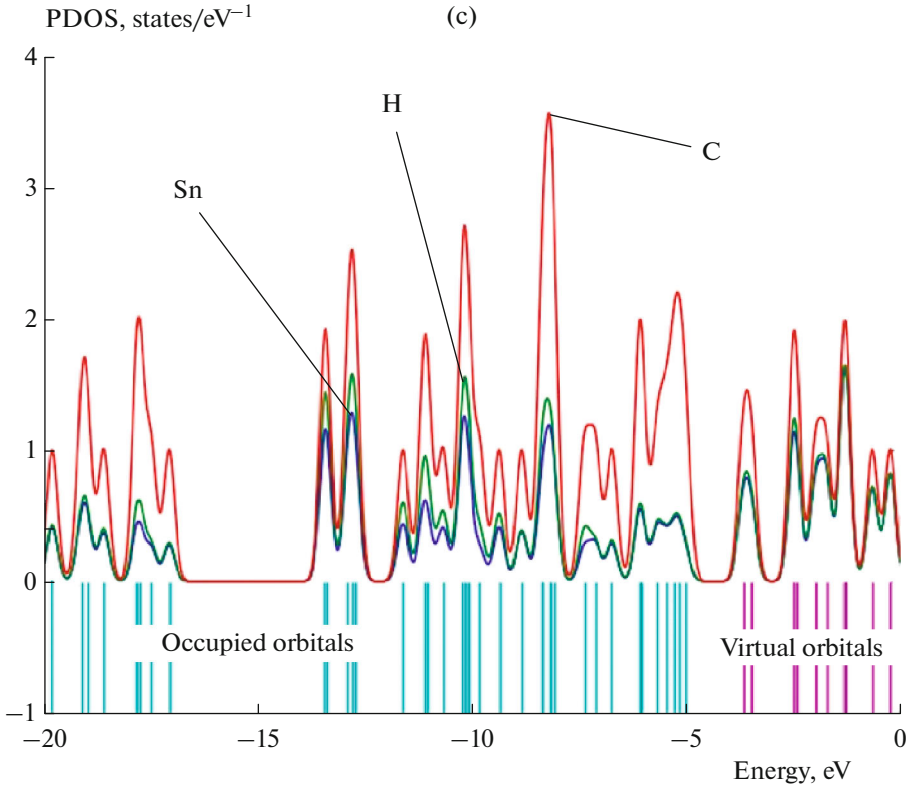
PDOS, states/eV^{-1}
(c)
H
C
Sn
Occupied orbitals
Virtual orbitals
Energy, eV
PDOS, states/eV^{-1}
(d)
H
Pb
C
Occupied orbitals
Virtual orbitals
Energy, eV

Fig. 2. (Contd.)

Table 1. The electric potential (E_p) and Bader charge (Q) for elements involved in the adsorption mechanism of 6H–adsorbed on the SiC, GeC, SnC and PbC nanocones using CAM-B3LYP/EPR-III, 6-311+G(d, p) calculation extracted of NQR method

Atom	Q	E_p	Atom	Q	E_p	Atom	Q	E_p	Atom	Q	E_p
SiC			GeC			SnC			PbC		
Si1	0.31	−48.58	Ge1	0.23	−153.98	Sn1	0.38	−284.14	Pb1	0.46	−1.62
Si2	0.58	−48.60	Ge2	0.48	−153.63	Sn2	0.64	−283.72	Pb2	0.14	−1.53
C3	−0.44	−14.69	C3	−0.37	−14.63	C3	−0.66	−14.73	C3	−0.91	−14.78
Si4	0.46	−48.49	Ge4	0.42	−153.91	Sn4	0.67	−284.06	Pb4	0.86	−1.58
Si5	0.35	−48.56	Ge5	0.33	−154.01	Sn5	0.48	−284.14	Pb5	0.62	−1.62
C6	−0.45	−14.72	C6	−0.40	−14.67	C6	−0.62	−14.74	C6	−0.89	−14.79
Si7	0.61	−48.43	Ge7	0.61	−153.91	Sn7	0.83	−284.05	Pb7	0.79	−1.56
C8	−0.66	−14.76	C8	−0.63	−14.68	C8	−0.74	−14.65	C8	0.03	−14.76
C9	−0.48	−14.72	C9	−0.43	−14.67	C9	−0.67	−14.76	C9	−0.75	−14.80
Si10	0.46	−48.49	Ge10	0.42	−153.91	Sn10	0.67	−284.06	Pb10	0.86	−1.58
Si11	0.31	−48.58	Ge11	0.23	−153.98	Sn11	0.38	−284.14	Pb11	0.46	−1.62
C12	−0.45	−14.72	C12	−0.40	−14.67	C12	−0.62	−14.74	C12	−0.89	−14.79
Si13	0.45	−48.50	Ge13	0.39	−153.94	Sn13	0.65	−284.08	Pb13	0.68	−1.59
C14	−0.48	−14.72	C14	−0.43	−14.67	C14	−0.67	−14.76	C14	−0.75	−14.80
C15	−0.31	−14.75	C15	−0.26	−14.71	C15	−0.45	−14.77	C15	−0.37	−14.76
Si16	0.45	−48.50	Ge16	0.39	−153.93	Sn16	0.65	−284.08	Pb16	0.68	−1.59
C17	−0.35	−14.77	C17	−0.29	−14.72	C17	−0.44	−14.76	C17	−0.52	−14.78
C18	−0.35	−14.77	C18	−0.29	−14.72	C18	−0.44	−14.76	C18	−0.52	−14.78
SiC–6H			GeC–6H			SnC–6H			PbC–6H		
Si1	0.43	−48.55	Ge1	0.34	−153.99	Sn1	0.57	−284.11	Pb1	0.52	−1.62
Si2	0.59	−48.62	Ge2	0.49	−153.637	Sn2	0.67	−283.74	Pb2	0.15	−1.55
C3	−0.44	−14.69	C3	−0.37	−14.6381	C3	−0.65	−14.75	C3	−0.92	−14.81
Si4	0.47	−48.52	Ge4	0.39	−153.941	Sn4	0.64	−284.08	Pb4	0.85	−1.60
Si5	0.46	−48.54	Ge5	0.35	−153.98	Sn5	0.60	−284.11	Pb5	0.63	−1.61
C6	−0.47	−14.75	C6	−0.41	−14.7029	C6	−0.65	−14.79	C6	−0.90	−14.82
Si7	0.63	−48.45	Ge7	0.60	−153.922	Sn7	0.86	−284.05	Pb7	0.73	−1.58
C8	−0.67	−14.76	C8	−0.63	−14.6887	C8	−0.75	−14.65	C8	0.03	−14.78
C9	−0.51	−14.73	C9	−0.46	−14.6975	C9	−0.69	−14.77	C9	−0.76	−14.81
Si10	0.47	−48.52	G10	0.39	−153.941	Sn10	0.64	−284.08	Pb10	0.85	−1.60
Si11	0.43	−48.55	Ge11	0.34	−153.99	Sn11	0.57	−284.11	Pb11	0.52	−1.62
C12	−0.47	−14.75	C12	−0.41	−14.7029	C12	−0.65	−14.79	C12	−0.90	−14.82
Si13	0.55	−48.50	Ge13	0.49	−153.976	Sn13	0.76	−284.10	Pb13	0.82	−1.60
C14	−0.51	−14.73	C14	−0.46	−14.6975	C14	−0.69	−14.77	C14	−0.76	−14.81
C15	−0.40	−14.72	C15	−0.38	−14.6938	C15	−0.57	−14.78	C15	−0.68	−14.80
Si16	0.55	−48.50	Ge16	0.49	−153.976	Sn16	0.76	−284.10	Pb16	0.82	−1.60
C17	−0.41	−14.71	C17	−0.36	−14.677	C17	−0.52	−14.74	C17	−0.71	−14.80
C18	−0.41	−14.71	C18	−0.36	−14.677	C18	−0.52	−14.74	C18	−0.71	−14.80
H19	−0.12	−1.24	H19	−0.08	−1.2055	H19	−0.15	−1.235	H19	−0.07	−1.09
H20	−0.12	−1.24	H20	−0.08	−1.1995	H20	−0.15	−1.22	H20	−0.06	−1.09
H21	−0.12	−1.24	H21	−0.08	−1.2055	H21	−0.15	−1.23	H21	−0.07	−1.09
H22	0.03	−1.17	H22	0.05	−1.1604	H22	0.03	−1.20	H22	0.20	−1.06
H23	0.03	−1.19	H23	0.05	−1.1689	H23	0.04	−1.20	H23	0.2043	−1.0864
H24	0.03	−1.19	H24	0.05	−1.1689	H24	0.04	−1.20	H24	0.2036	−1.0864

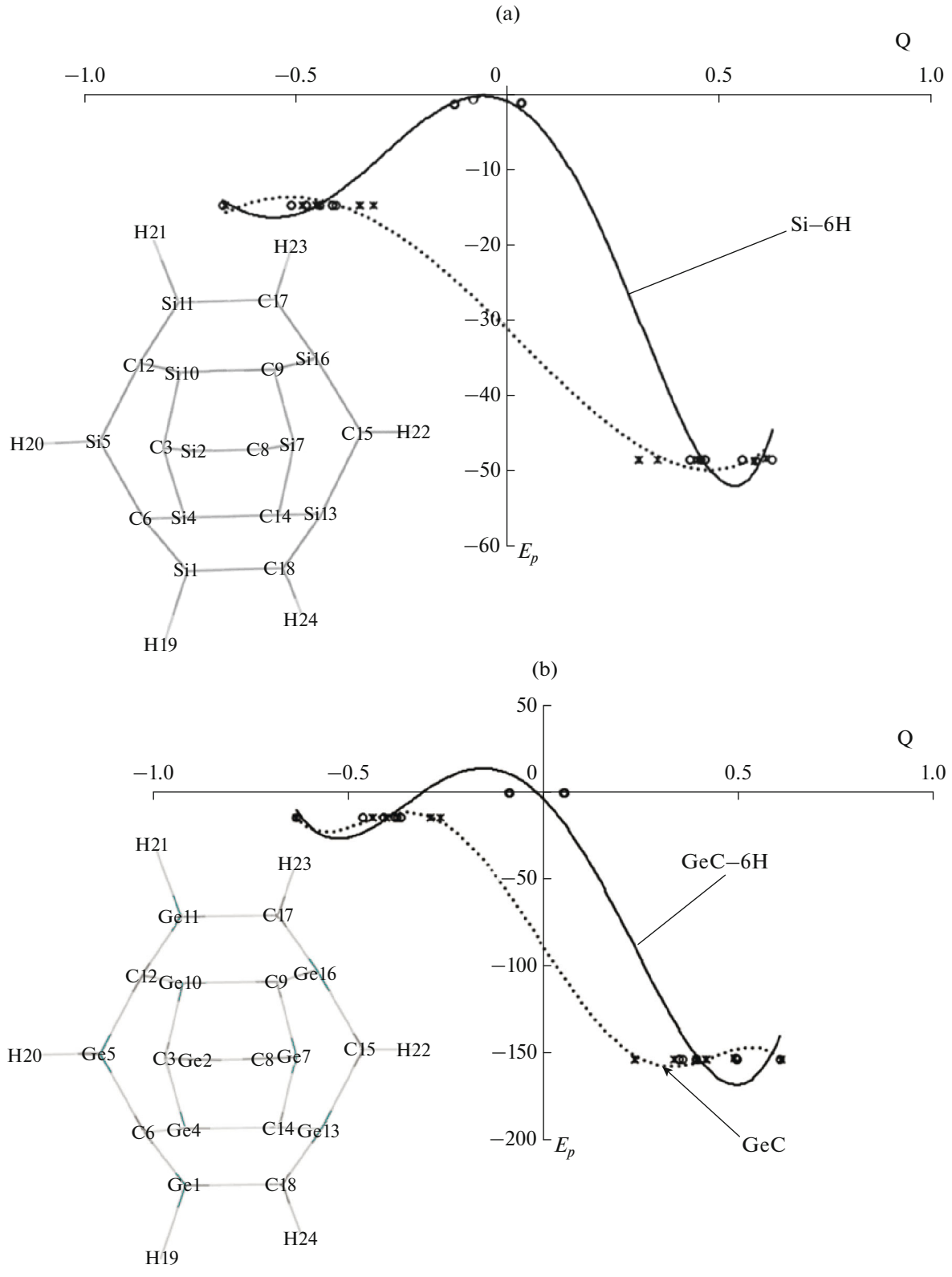

Fig. 3. The electric potential (a.u.) versus Bader charge (Coulomb) through NQR calculation for (a) SiC, SiC–6H, (b) GeC, GeC–6H, (c) SnC, SnC–6H, and (d) PbC, PbC–6H nanocones by using CAM-B3LYP/EPR-III, LANL2DZ,6–311+G(*d*, *p*)**.** (Note: dotted line for SiC, GeC, SnC and PbC and dash line for SiC–6H, GeC–6H, SnC–6H, and PbC–6H nanocone hydrides).

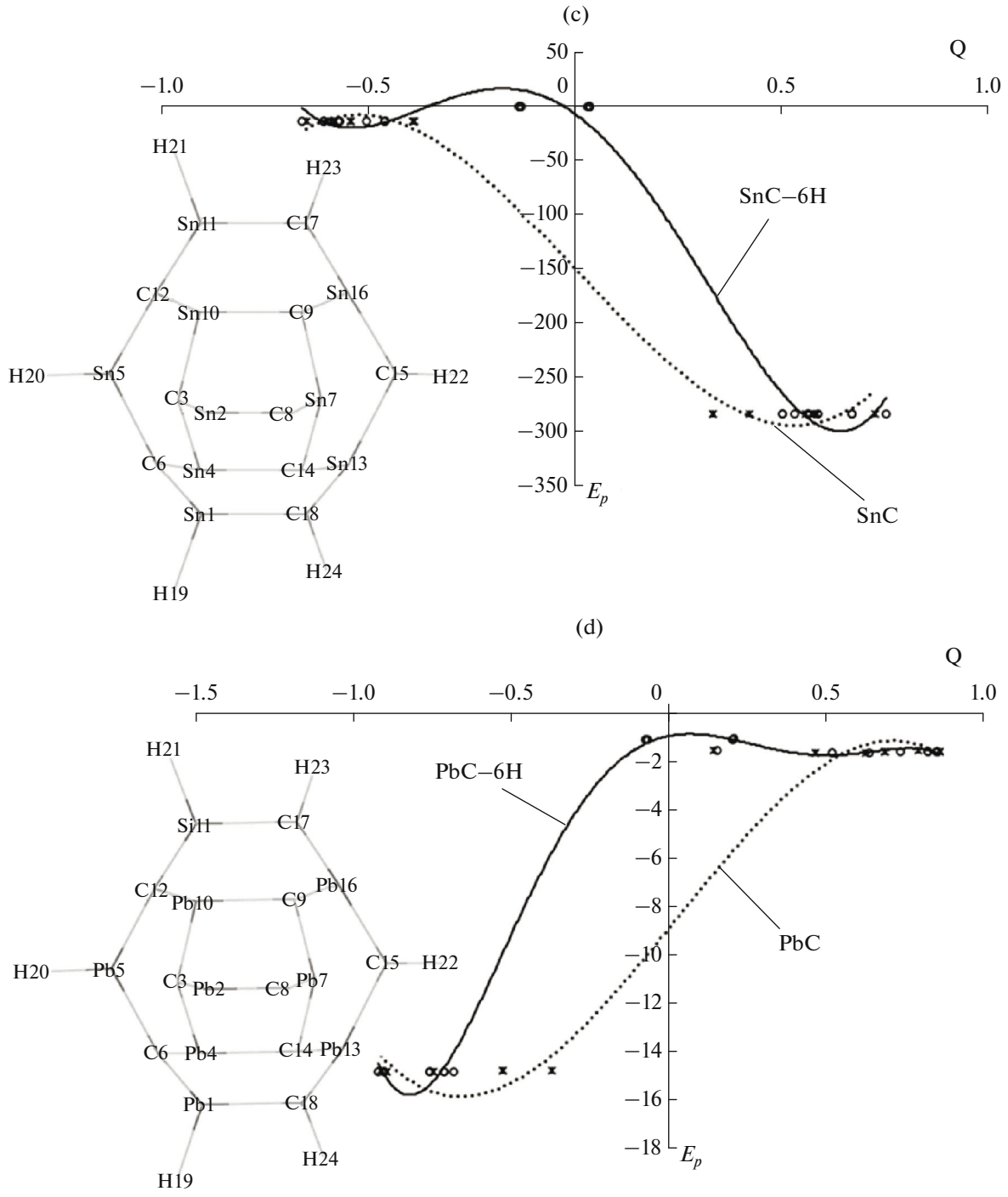

Fig. 3. (Contd.)

hydrides have been calculated using Gaussian 16, Revision C.01 and reported in Table 2 [48].

The resulted graphs of NMR data in Figs. 4a–4d have shown approximately the identical chemical shielding behavior of isotropic and anisotropy factors of SiC, GeC, SnC, PbC and SiC–6H, GeC–6H, SnC–6H, PbC–6H nanocones with several sharp peaks related to carbon, silicon, germanium, tin and lead (adsorbent) and hydrogen atoms (adsorbate) in the active site situations [68, 69]. Several sharp peaks related to the adsorption site of atoms including C6, C12 for SiC–6H; Ge2, Ge5, Ge7, Ge10, Ge13, Ge16 for GeC–6H; Sn2 for SnC–6H; and C3, C6, C8, C12 for PbC–6H nanocones, respectively, have been exhibited (Figs. 4a–4d).

Table 2. Data of GIAO/NMR shielding tensors for selected atoms of 6H–adsorbed on the SiC, GeC, SnC and PbC nanocones using CAM-B3LYP/EPR-III, 6-311+G (*d*, *p*), LANL2DZ calculation

Atom	σ_{iso}	σ_{aniso}	Atom	σ_{iso}	σ_{aniso}	Atom	σ_{iso}	σ_{aniso}	Atom	σ_{iso}	σ_{aniso}
SiC			GeC			SnC			PbC		
Si1	1852.89	9277.86	Ge1	524.26	4076.84	Sn1	3852.47	1253.86	Pb1	8.31	81.00
Si2	707.19	1372.55	Ge2	2938.45	1816.30	Sn2	4488.45	630.72	Pb2	21.07	19.94
C3	26.33	1184.71	C3	1055.13	1882.32	C3	692.28	2220.56	C3	337.21	1607.15
Si4	396.87	636.05	Ge4	1995.87	1646.88	Sn4	4033.85	734.59	Pb4	1.87	35.74
Si5	751.30	5584.16	Ge5	1063.43	2074.33	Sn5	3660.39	1122.08	Pb5	33.60	62.80
C6	180.18	6093.06	C6	517.81	2231.17	C6	117.54	651.14	C6	615.75	2721.27
Si7	44.56	1523.67	Ge7	1817.70	1660.13	Sn7	3631.00	1598.10	Pb7	19.15	58.84
C8	62.57	392.10	C8	54.39	223.00	C8	114.31	171.10	C8	184.82	320.20
C9	334.25	1328.91	C9	250.62	776.38	C9	192.36	634.91	C9	61.98	889.56
Si10	396.87	636.05	Ge10	1995.87	1646.88	Sn10	4033.85	734.59	Pb10	1.87	35.74
Si11	1852.89	9277.86	Ge11	524.26	4076.84	Sn11	3852.47	1253.86	Pb11	8.31	81.00
C12	180.18	6093.06	C12	517.81	2231.17	C12	117.54	651.14	C12	615.75	2721.27
Si13	758.72	5091.88	Ge13	1064.28	1824.86	Sn13	4274.51	544.97	Pb13	17.52	27.08
C14	334.25	1328.91	C14	250.62	776.38	C14	192.36	634.91	C14	61.98	889.56
C15	215.44	2129.14	C15	451.46	2033.64	C15	677.30	2314.08	C15	492.25	3669.89
Si16	758.72	5091.88	Ge16	1064.28	1824.86	Sn16	4274.51	544.97	Pb16	17.52	27.08
C17	6842.22	11517.20	C17	2301.78	5664.74	C17	992.37	2612.59	C17	523.30	3890.65
C18	6842.22	11517.20	C18	2301.78	5664.74	C18	992.37	2612.59	C18	523.30	3890.65
SiC–6H			GeC–6H			SnC–6H			PbC–6H		
Si1	652.10	2043.44	Ge1	1685.95	995.58	Sn1	5331.11	3908.81	Pb1	12.36	13.20
Si2	578.88	1376.18	Ge2	2046.74	677.24	Sn2	8048.78	12679.47	Pb2	20.98	15.84
C3	328.76	1145.67	C3	45.41	593.36	C3	3086.70	9101.54	C3	131.05	958.87
Si4	939.44	1737.45	Ge4	1943.38	1109.69	Sn4	5625.13	9355.57	Pb4	9.36	21.06
Si5	787.04	1304.99	Ge5	2694.16	2627.14	Sn5	7373.91	4446.71	Pb5	12.51	24.91
C6	1995.05	4581.12	C6	398.11	1004.59	C6	1601.63	4860.79	C6	448.32	912.92
Si7	112.75	579.31	Ge7	1618.75	555.21	Sn7	11387.79	22754.53	Pb7	20.40	17.74
C8	269.51	621.86	C8	6.13	304.30	C8	6947.47	10490.25	C8	510.55	949.44
C9	624.36	2381.21	C9	73.41	442.04	C9	419.87	2370.50	C9	113.43	520.46
Si10	939.44	1737.45	G10	1943.38	1109.69	Sn10	5625.13	9355.57	Pb10	9.25	21.08
Si11	652.10	2043.44	Ge11	1685.95	995.58	Sn11	5331.11	3908.81	Pb11	12.23	13.18
C12	1995.05	4581.12	C12	398.11	1004.59	C12	1601.63	4860.79	C12	446.51	899.43
Si13	428.68	428.68	Ge13	2199.69	1909.55	Sn13	2735.23	3523.36	Pb13	8.09	13.00
C14	624.36	2381.21	C14	73.41	442.04	C14	419.87	2370.50	C14	115.24	523.12
C15	434.84	933.74	C15	308.33	606.65	C15	1362.97	2901.56	C15	266.78	599.45
Si16	428.68	678.29	Ge16	2199.69	1909.55	Sn16	2735.23	3523.36	Pb16	8.08	12.86
C17	3.30	424.80	C17	29.31	277.52	C17	125.32	949.53	C17	109.60	357.95
C18	3.30	424.80	C18	29.31	277.52	C18	125.32	949.53	C18	109.53	356.45
H19	35.71	53.79	H19	28.76	15.32	H19	29.60	44.09	H19	24.84	9.30
H20	22.72	19.10	H20	28.54	18.06	H20	24.69	11.31	H20	23.64	8.60
H21	35.71	53.79	H21	28.76	15.32	H21	29.60	44.09	H21	24.50	8.96
H22	45.58	57.70	H22	41.00	48.39	H22	60.61	70.10	H22	39.94	42.28
H23	18.34	13.91	H23	21.09	11.75	H23	0.82	61.14	H23	18.31	16.50
H24	18.34	13.91	H24	21.09	11.75	H24	0.82	61.14	H24	18.30	16.39

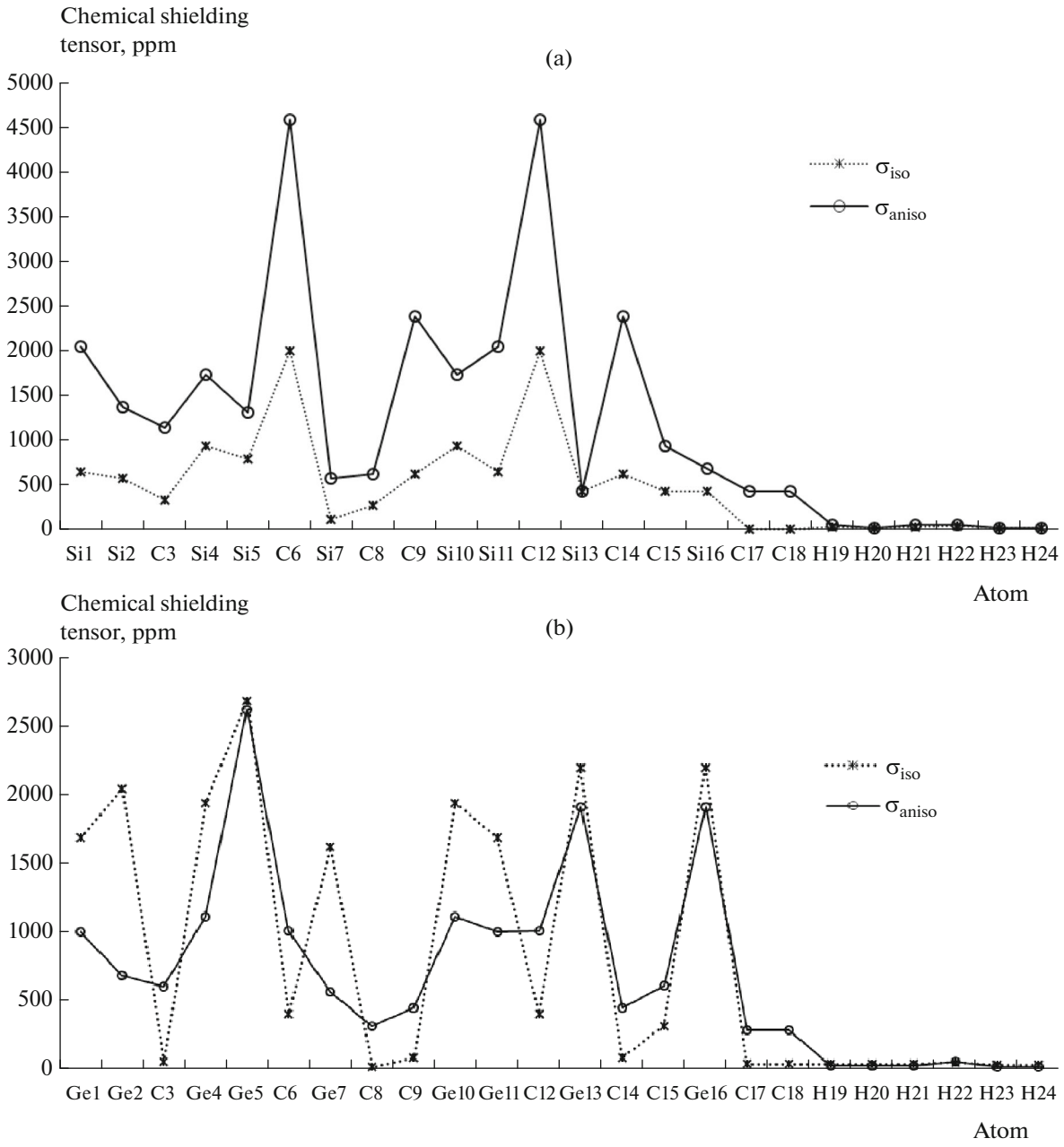

Fig. 4. Chemical shielding tensors (ppm) of isotropic (σ_{iso}) and anisotropy (σ_{aniso}) extract from NMR spectrums for (a) SiC–6H, (b) GeC–6H, (c) SnC–6H, and (d) PbC–6H nanocone hydrides.

Infrared Spectra of 6H-adsorption Onto Nanocone Carbides

Thermodynamic characters were evaluated for hydrogen on the surface of SiC, GeC, SnC and PbC nanocones as gas detectors which can be applicable as selective sensors for hydrogen storage (Table 3). Furthermore, the infrared spectrums for adsorption of hydrogen atoms on the surface of SiC, GeC, SnC and PbC nanocones have been reported in Figs. 5a–5d. The graph of SiC–6H complex has been observed in the frequency range between 500–2500 cm^{-1} with sharp peaks around 815.93 and 227.03 cm^{-1}. The graph of GeC–6H complex has been observed in the frequency range between 500–1000 cm^{-1} with strong peaks around 588.37 and 777.77 cm^{-1}. The graph of SnC–6H complex has been observed in the frequency range between 250–1250 cm^{-1} with strong peaks around 393.08 and 761.38 cm^{-1}. Finally, the graph of PbC–6H complex has been observed in the frequency range between 1500–2500 cm^{-1} with strong peaks around 182.37 and 1515.14 cm^{-1}.

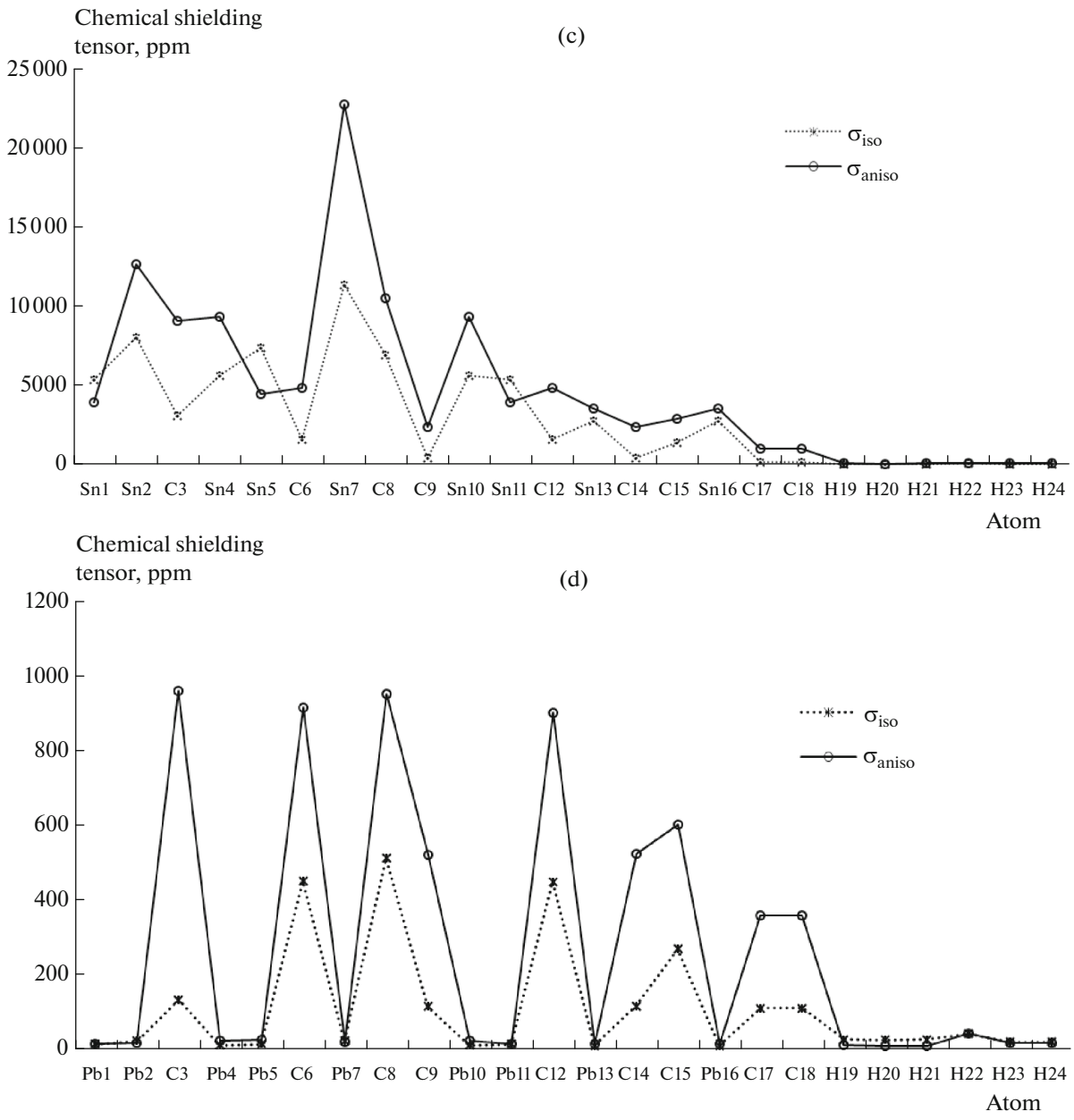

Fig. 4. (Contd.)

The adsorptive capacity of hydrogen on the surface of SiC, GeC, SnC and PbC nanocones is approved by the ΔE^{o}_{ads} amounts as formula:

$$\Delta E^{o}_{ads} = \Delta E^{o}_{6H\to XC} - \left(\Delta E^{o}_{6H} + \Delta E^{o}_{XC}\right), \quad (X = \text{Si, Ge, Sn, Pb}). \quad (1)$$

Furthermore, the difference of ΔH^{o}_{ads} among adsorption of hydrogen atoms on the surface of SiC, GeC, SnC and PbC structures have been unraveled due to noncovalent binding resulted from interatomic interactions between hydrogen atoms and surface of SiC, GeC, SnC and PbC structures and covalent binding resulted from intra-atomic interactions between carbon, silicon, germanium, tin and lead in nanocone (Table 3). In fact, SiC, GeC, SnC and PbC nanocones have higher interaction energy from Van der Waals' forces with hydrogen atoms that can make them highly stable.

For the adsorption mechanism, ΔG^{o}_{ads} is calculated as follows:

$$\Delta G^{o}_{ads} = \Delta G^{o}_{6H\to XC} - \left(\Delta G^{o}_{6H} + \Delta G^{o}_{XC}\right), \quad (X = \text{Si, Ge, Sn, Pb}). \quad (2)$$

Table 3. The thermodynamic character of SiC, GeC, SnC, PbC nanocones and SiC–6H, GeC–6H, SnC–6H, and PbC–6H nanocone hydrides

6H–adsorbed on Nanocones	$\Delta E^{o} \times 10^{-4}$, kcal/mol	$\Delta H^{o} \times 10^{-4}$, kcal/mol	$\Delta G^{o} \times 10^{-4}$, kcal/mol	S^{o}, cal/K mol	Dipole moment, Debye
SiC	−182.7474	−182.7474	−182.7514	134.576	4.1234
GeC	−1180.6421	−1180.6421	−1180.6465	148.277	3.3993
PbC	−23.3096	−23.3095	−23.3132	123.440	8.6603
SiC–6H	−182.9776	−182.9775	−182.9815	132.507	2.3194
GeC–6H	−1180.8751	−1180.8750	−1180.8798	161.024	1.4991
SnC–6H	−3390.3269	−3390.3269	−3390.3316	157.153	2.1738
PbC–6H	−23.5365	−23.5365	−23.5405	136.838	3.1099

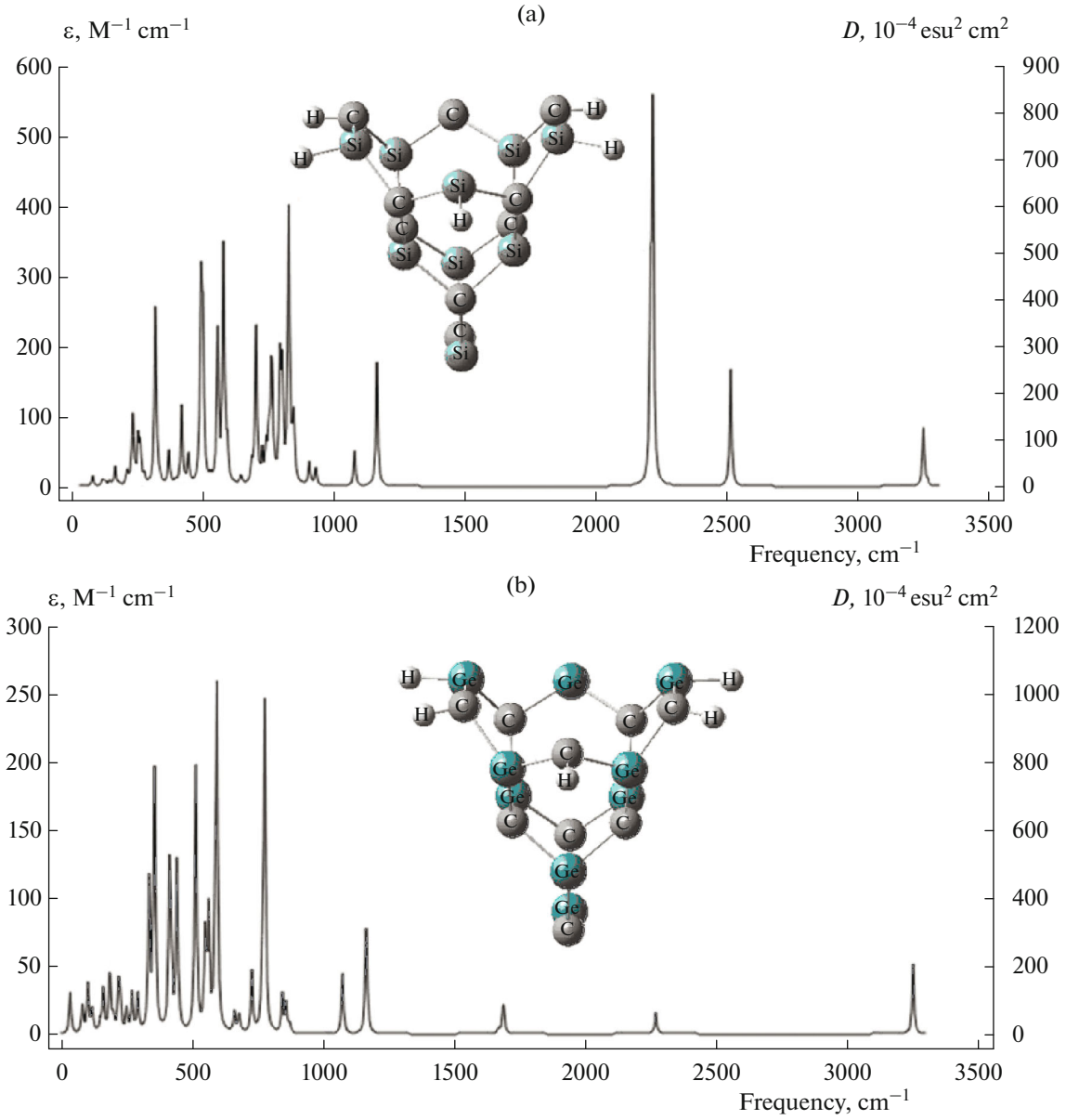

Fig. 5. The frequency (cm^{-1}) changes through the IR spectrums for (a) SiC–6H, (b) GeC–6H, (c) SnC–6H, and (d) PbC–6H nanocone hydrides as the selective gas detectors [Note: ε (M^{-1} cm^{-1}) is the absorbance unit and D (10^{-4} esu^2 cm^2) is the dipole strength via the esu or electrostatic unit, which is a unit of charge in the cgs (centimeter-gram-second system)].

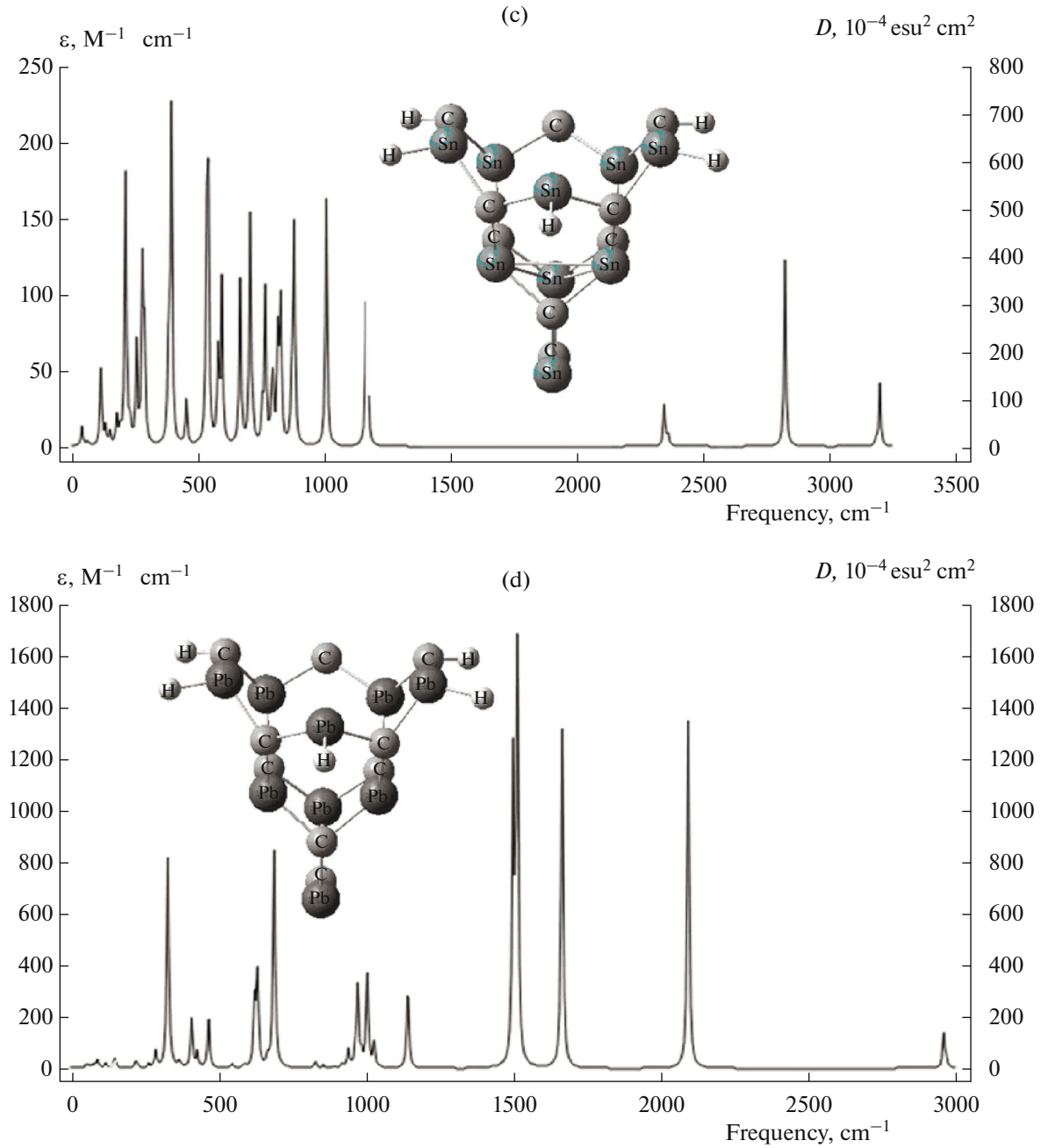

Fig. 5. (Contd.)

As shown in Table 3, all the computed ΔG^{o}_{ads} amounts are close, which exhibits the accord of the evaluated data by all methods and the validity of the computations. In addition, the results of Table 3 has indicated that SiC–6H, GeC–6H, SnC–6H, PbC–6H nanocone hydrides have the largest gap of Gibbs free energy adsorption with which defines the changes between Gibbs free energy of initial compounds (ΔG^{o}_{6H}) and (ΔG^{o}_{SiC}, ΔG^{o}_{GeC}, ΔG^{o}_{SnC}, ΔG^{o}_{PbC}) and product compounds (ΔG^{o}_{SiC-6H}, ΔG^{o}_{GeC-6H}, ΔG^{o}_{SnC-6H}, ΔG^{o}_{PbC-6H}) through polarizability.

However, SiC, GeC, SnC and PbC nanocones seem to possess enough efficiency for adsorption of hydrogen atoms through charge transfer from hydrogen to carbon, silicon, germanium, tin and lead due to intra-atomic and interatomic interactions. From the magnitude results of the adsorption energies, it was derived that the hydrogen was chemisorbed on SiC and GeC, while the detecting was physical in nature

on the SnC and PbC nanocones. Overall analysis showed that SiC and GeC nanocones indicated better interactions and therefore, better detecting of hydrogen compared to the other carbides.

CONCLUSIONS

Hydrogen adsorbed SiC, GeC, SnC and PbC nanocones have been studied by first-principle calculations. The values of changes of charge density have shown a more important charge transfer for SiC, GeC, SnC and PbC nanocones which act as the electron acceptor while hydrogen atoms act as the stronger electron donner through adsorption on the SiC, GeC, SnC and PbC nanocones. In fact, SiC–6H, GeC–6H, SnC–6H, and PbC–6H nanocone hydrides have higher interaction energy from Van der Waals' forces with hydrogen atoms that can make them highly stable.

Moreover, a thermodynamic formalism describing adsorption processes of hydrogen atoms on the solid adsorbent of SiC, GeC, SnC and PbC nanocones has been developed. Besides, this process is being treated as an internal process of the absorbent–adsorbate system. Thermodynamic parameters have constructed a detailed molecular model for atom–atom interactions and a distribution of point charges is used to reproduce the polarity of the solid material and the adsorbing molecules.

ACKNOWLEDGMENTS

In successfully completing this paper and its research, the authors are grateful to Kastamonu University.

FUNDING

This work was supported by ongoing institutional funding. No additional grants to carry out or direct this particular research were obtained.

CONFLICT OF INTEREST

The authors of this work declare that they have no conflicts of interest.

REFERENCES

1. S. Bagheri, M. Monajjemi, A. Ziglari, et al., Russ. J. Phys. Chem. B **15** (Suppl. 1), S140–S148 (2021). https://doi.org/10.1134/S1990793121090049
2. D. N. Polyakov, V. V. Shumova, and L. M. Vasilyak, Russ. J. Phys. Chem. B **17**, 1241–1245 (2023). https://doi.org/10.1134/S1990793123050263
3. B. S. Seplyarskii, R. A. Kochetkov, T. G. Lisina, et al., Russ. J. Phys. Chem. B **17**, 1098–1105 (2023). https://doi.org/10.1134/S199079312305010X
4. E. I. Rudenko, N. V. Dohlikova, A. K. Gatin, et al., Russ. J. Phys. Chem. B **17**, 845–852 (2023). https://doi.org/10.1134/S1990793123040164
5. M. A. A. Zadeh, H. Lari, L. Kharghanian, et al., J. Comput. Theor. Nanosci. **12**, 4358 (2015). https://doi.org/10.1166/jctn.2015.4366
6. M. Monajjemi, M. Khaleghian, N. Tadayonpour, et al., Int. J. Nanosci. **9**, 517–529 (2010). https://doi.org/10.1142/S0219581X10007071
7. B. Khalili Hadad, F. Mollaamin, and M. Monajjemi, Russ. Chem. Bull. **60**, 238–241 (2011). https://doi.org/10.1007/s11172-011-0039-5
8. F. Mollaamin and M. Monajjemi, Mol. Simul. **49**, 365 (2023). https://doi.org/10.1080/08927022.2022.2159996
9. F. Mollaamin and M. Monajjemi, Sensor Rev. 43, 266–279 (2023). https://doi.org/10.1108/SR-03-2023-0040
10. M. Monajjemi, F. Mollaamin, and S. Shojaei, Biointerface Res. Appl. Chem. 10, 5575 (2020). https://doi.org/10.33263/BRIAC103.575585
11. F. Mollaamin and M. Monajjemi, Appl. Chem. Eng. **6**, 1–14 (2023). https://doi.org/10.24294/ace.v6i2.2199
12. E. A. Neskoromnaya, A. V. Babkin, E. A. Zakharchenko, et al., Russ. J. Phys. Chem. B **17**, 818–825 (2023). https://doi.org/10.1134/S1990793123040139
13. K. Geim, Science **324**, 1530–1534 (2009). https://doi.org/10.1126/science.115887
14. A. H. Castro Neto, F. Guinea, N. M. R. Peres, et al., Rev. Mod. Phys. **81**, 109–162 (2009). https://doi.org/10.1103/RevModPhys.81.109
15. L. I. Trakhtenberg, Russ. J. Phys. Chem. B **17**, 600–607 (2023). https://doi.org/10.1134/S1990793123030144
16. M. Monajjemi, F. Mollaamin, M. R. Gholami, et al., Main Group Met. Chem. **26**, 349 (2003). https://doi.org/10.1515/MGMC.2003.26.6.349
17. F. Mollaamin and M. Monajjemi, J. Mol. Model. **29**, 170 (2023). https://doi.org/10.1007/s00894-023-05567-8
18. M. Monajjemi, M. T. Baie, and F. Mollaamin, Russ. Chem. Bull. **59**, 886–889 (2010). https://doi.org/10.1007/s11172-010-0181-5
19. F. Mollaamin, M. Monajjemi, S. Salemi, et al., Fuller. Nanotub. Carbon Nanostruct. **19**, 182 (2011). https://doi.org/10.1080/15363831003782932
20. F. Mollaamin and M. Monajjemi, J. Clust. Sci. **34**, 2901 (2023). https://doi.org/10.1007/s10876-023-02436-5
21. F. Mollaamin and M. Monajjemi, C.-J. Carbon Res. **9**, 20 (2023). doi
22. F. Mollaamin, S. Shahriari, M. Monajjemi, et al., J. Clust. Sci. **34**, 1547–1562 (2023). https://doi.org/10.1007/s10876-022-02335-1
23. F. Mollaamin and M. Monajjemi, Clean Technol. **5**, 403–417 (2023). https://doi.org/10.3390/cleantechnol5010020
24. F. Mollaamin and M. Monajjemi, J. Mol. Model. **29**, 119 (2023). https://doi.org/10.1007/s00894-023-05526-3
25. F. Mollaamin, Appl. Chem. Eng. **6**, 1–14 (2023). https://doi.org/10.24294/ace.v6i3.2303

26. A. E. Galashev, Russ. J. Phys. Chem. B **17**, 113–121 (2023). https://doi.org/10.1134/S1990793123010190
27. L. Lin, Y. Chen, L. Yao, et al., J. Luminescence **239**, 118341 (2021). https://doi.org/10.1016/j.jlumin.2021.118341
28. Y. Wu, L. P. Zhou, X. Z. Du, et al., J. Nanosci. Nanotech. **15**, 3017–3024 (2015). https://doi.org/10.1166/jnn.2015.9687
29. E. Bekaroglu, M. Topsakal, S. Cahagirov, et al., Phys. Rev. B **81**, 075433–075441 (2010). https://doi.org/10.1103/PhysRevB.81.075433
30. N. Alaal, V. Loganathan, N. Medhekar, et al., J. Phys. D: Appl. Phys. **49**, 105306–105314 (2016). https://doi.org/10.1088/0022-3727/49/10/105306
31. K. J. Kim and Y. W. Kim, J. Eur. Ceram. Soc. **32**, 1149–1155 (2012). https://doi.org/10.1016/j.jeurceramsoc.2011.11.037
32. N. V. Dokhlikova, S. A. Ozerin, S. V. Doronin, et al., Russ. J. Phys. Chem. B **16**, 461–467 (2022). https://doi.org/10.1134/S1990793122030137
33. V. B. Merinov and V. A. Domnin, Russ. J. Phys. Chem. B **17**, 215–221 (2023). https://doi.org/10.1134/S1990793123010268
34. N. V. Dokhlikova, A. K. Gatin, S. Y. Sarvadiy, et al., Russ. J. Phys. Chem. B **16**, 772–779 (2022). https://doi.org/10.1134/S1990793122040042
35. K. Y. Troshin, N. M. Rubtsov, G. I. Tsvetkov, et al., Russ. J. Phys. Chem. B **16**, 693–698 (2022). https://doi.org/10.1134/S1990793122040303
36. A. E. Smygalina and A. D. Kiverin, Russ. J. Phys. Chem. B **17**, 907–914 (2023). https://doi.org/10.1134/S1990793123040188
37. M. A. Kotov, S. Y. Lavrentyev, N. G. Solovyov, et al., Russ. J. Phys. Chem. B **17**, 953–961 (2023). https://doi.org/10.1134/S1990793123040267
38. A. M. Tereza, G. L. Agafonov, E. K. Anderzhanov, et al., Russ. J. Phys. Chem. B **17**, 974–978 (2023). https://doi.org/10.1134/S1990793123040309
39. K. Y. Troshin, N. M. Rubtsov, G. I. Tsvetkov, et al., Russ. J. Phys. Chem. B **17**, 979–985 (2023). https://doi.org/10.1134/S1990793123040310
40. A. H. Davtyan, Z. O. Manukyan, S. D. Arsentev, et al., Russ. J. Phys. Chem. B **17**, 336–345 (2023). https://doi.org/10.1134/S1990793123020239
41. V. Y. Agroskin, B. G. Bravy, G. K. Vasiliev, et al., Russ. J. Phys. Chem. B **16**, 596–601 (2022). https://doi.org/10.1134/S1990793122040029
42. A. M. Tereza, G. L. Agafonov, E. K. Anderzhanov, et al., Russ. J. Phys. Chem. B **17**, 425–432 (2023). https://doi.org/10.1134/S1990793123020173
43. K. Y. Troshin, N. M. Rubtsov, G. I. Tsvetkov, et al., Russ. J. Phys. Chem. B **17**, 433–438 (2023). https://doi.org/10.1134/S1990793123020185
44. Y. Miyamoto and B. D. Yu, Appl. Phys. Lett. **80**, 586e8 (2002). https://doi.org/10.1063/1.1445474
45. F. Mollaamin, A. Ilkhani, N. Sakhaei, et al., J. Comput. Theor. Nanosci. **12**, 3148–3154 (2015). https://doi.org/10.1166/jctn.2015.4092
46. F. Mollaamin and M. Monajjemi, Russ. J. Phys. Chem. **97**, 2241 (2023). https://doi.org/10.1134/S0036024423100096
47. R. Dennington, T. A. Keith, and J. M. Millam, *GaussView, Version 6.06.16* (Semichem Inc., Shawnee Mission, KS, 2016).
48. M. J. Frisch, G. W. Trucks, H. B. Schlegel, G. E. Scuseria, M. A. Robb, J. R. Cheeseman, G. Scalmani, V. Barone, G. A. Petersson, H. Nakatsuji, X. Li, M. Caricato, A. V. Marenich, J. Bloino, B. G. Janesko, R. Gomperts, B. Mennucci, H. P. Hratchian, J. V. Ortiz, A. F. Izmaylov, J. L. Sonnenberg, D. Williams-Young, F. Ding, F. Lipparini, F. Egidi, J. Goings, B. Peng, A. Petrone, T. Henderson, D. Ranasinghe, V. G. Zakrzewski, J. Gao, N. Rega, G. Zheng, W. Liang, M. Hada, M. Ehara, K. Toyota, R. Fukuda, J. Hasegawa, M. Ishida, T. Nakajima, Y. Honda, O. Kitao, H. Nakai, T. Vreven, K. Throssell, J. A. Montgomery, Jr., J. E. Peralta, F. Ogliaro, M. J. Bearpark, J. J. Heyd, E. N. Brothers, K. N. Kudin, V. N. Staroverov, T. A. Keith, R. Kobayashi, J. Normand, K. Raghavachari, A. P. Rendell, J. C. Burant, S. S. Iyengar, J. Tomasi, M. Cossi, J. M. Millam, M. Klene, C. Adamo, R. Cammi, J. W. Ochterski, R. L. Martin, K. Morokuma, O. Farkas, J. B. Foresman, and D. J. Fox, *Gaussian 16, Revision C.01* (Gaussian, Inc., Wallingford CT, 2016).
49. J. P. Perdew, K. Burke, and M. Ernzerhof, Phys. Rev. Lett. **77**, 3865 (1996). https://doi.org/10.1103/PhysRevLett.77.3865
50. F. Mollaamin and M. Monajjemi, Computation 11, 108 (2023). https://doi.org/10.3390/computation11060108
51. K. Bakhshi, F. Mollaamin, and M. Monajjemi, J. Comput. Theor. Nanosci. **8**, 763–768 (2011). https://doi.org/10.1166/jctn.2011.1750
52. Zy. Chen, and Jl. Yang, Front. Phys. China **1**, 339–343 (2006). https://doi.org/10.1007/s11467-006-0026-8
53. T. Yanai, D. P. Tew, and N. C. Handy, Chem. Phys. Lett. **393**, 51–57 (2004). https://doi.org/10.1016/j.cplett.2004.06.011
54. M. P. Bircher and U. Rothlisberger, J. Chem. Theory Comput. **14**, 3184–3195 (2018). https://doi.org/10.1021/acs.jctc.8b00069
55. M. Khaleghian, M. Zahmatkesh, F. Mollaamin, et al., Fuller. Nanotub. Carbon Nanostruct. **19**, 251–261 (2011). https://doi.org/10.1080/15363831003721757
56. M. Monajjemi, M. Noei, and F. Mollaamin, Nucleos. Nucleot. Nucl. **29**, 676–683 (2010). https://doi.org/10.1080/15257771003781642
57. A. Tahan, F. Mollaamin, and M. Monajjemi, Russ. J. Phys. Chem. **83**, 587–597 (2009). https://doi.org/10.1134/S003602440904013X
58. F. Mollaamin and M. Monajjemi, Russ. J. Phys. Chem. B **17**, 658 (2023). https://doi.org/10.1134/S1990793123030223
59. B. Esfandiari, F. Mollaamin, M. Monajjemi, M., et al., Russ. J. Phys. Chem. B **17**, 1069–1082 (2023). https://doi.org/10.1134/S1990793123050196

60. G. Henkelman, A. Arnaldsson, and H. Jónsson, Comput. Mater. Sci. **36**, 354–360 (2006). https://doi.org/10.1016/j.commatsci.2005.04.010
61. N. V. Dokhlikova, A. K. Gatin, S. Y. Sarvadiy, et al., Russ. J. Phys. Chem. B **15**, 732–739 (2021). https://doi.org/10.1134/S1990793121040023
62. O. A. Kim, T. V. Bogdan, A. E. Koklin, et al., Russ. J. Phys. Chem. B **16**, 1218–1220 (2022). https://doi.org/10.1134/S1990793122070107
63. N. Job and K. Thirumoorthy, J. Phys. Chem. A **126**, 9366–9374 (2022). https://doi.org/10.1021/acs.jpca.2c06230
64. J. A. S. Smith, J. Chem. Educ. **48**, 39–41 (1971).
65. L. Piveteau, V. Morad, and M. V. Kovalenko, J. Am. Chem. Soc. **142**, 19413–19437 (2020). https://doi.org/10.1021/jacs.0c07338
66. Z. Trontelj, J. Pirnat, V. Jazbinšek, et al., Crystals **10**, 450 (2020). https://doi.org/10.3390/cryst10060450
67. H. A. Young and R. D. Freedman, *Sears and Zemansky's University Physics with Modern Physics*, 13th ed. (Addison-Wesley, Boston, 2012), p. 754.
68. S. N. Kozlov and B. E. Zhestkov, Russ. J. Phys. Chem. B **16**, 1030–1037 (2022). https://doi.org/10.1134/S1990793122060069
69. E. A. Salgansky, M. V. Tsvetkov, Y. Y. Tsvetkova, et al., Russ. J. Phys. Chem. B **16**, 1085–1091 (2022). https://doi.org/10.1134/S1990793122060100